

PREDICTING THE LONG-TERM FAILURE OF POLYCARBONATE: A CONSTITUTIVE APPROACH

E.T.J. KLOMPEN, T.A.P. ENGELS, R.P.M. JANSSEN, L.E. GOVAERT, H.E.H. MEIJER
Dutch Polymer Institute (DPI), Materials Technology (Mate)
Eindhoven University of Technology, Eindhoven, The Netherlands

ABSTRACT

In this study, an in-house numerical model is employed to predict the time-to-failure of polycarbonate under long-term constant or cyclic loading. This elasto-viscoplastic model captures the intrinsic deformation behavior of the glassy polymer. The model parameters are determined from uni-axial compression testing. In the case of long-term loading, however, special attention should be given to the intrinsic deformation behavior, as this might change within the time-scale of the experiment. Therefore, an elaborate investigation is performed to implement so-called aging kinetics in this model. It is shown that the application of approach leads to accurate predictions of time-to-failure under both constant loading and cyclic loading conditions. Moreover, the current model is based on a single parameter set and is molecular weight independent.

1 INTRODUCTION

Over the past 15 years substantial attention is drawn to the development of constitutive relations focusing on strain localization phenomena [1–5]. From this constitutive modeling it became apparent that the thermal history of a polymer strongly affects the macroscopic deformation behavior of the polymer. It showed that strain localization phenomena stem from the amount of intrinsic strain softening, whereas the intrinsic strain hardening behavior proved to have a stabilizing effect on the localized zones. This interaction between localization and stabilization of the localized zones eventually defines whether the polymer deforms macroscopically ductile or brittle [6]. Van Melick has already proved to predict effectively the strain localization of glassy polymers during (short-term) uni-axial tensile testing [6], using the elasto-viscoplastic constitutive model as reported by Govaert [5]. The model parameters are determined by compression testing. In this way, the intrinsic deformation can be obtained, as then localization phenomena are absent. Since similar localization phenomena are also observed for long-term static and cyclic loading conditions, the same numerical approach is applied to predict the time-to-failure under these conditions. Concerning the application to long-term loading conditions, one should consider the effect of progressive aging [7], which might change material parameters within the experimental time-scale. Due to this aging effect, the intrinsic material properties (yield stress and thus strain softening) alter throughout the experiment. These time-dependent intrinsic properties, on its turn, have a strong effect on the failure behavior of polymers under long-term loading. For this reason, a modification of the elasto-viscoplastic constitutive model is proposed to account for changes in intrinsic behavior during long-term loading [8].

2 EXPERIMENTAL METHODS

Cylindrical samples of $\text{Ø}6 \times 6 \text{mm}$ were machined to perform uni-axial compression tests. The samples were compressed on a servo-hydraulic MTS Elastomer Testing System 810 between two parallel, flat steel plates. The tests were performed at constant true strain rates of 10^{-4} s^{-1} to 10^{-2} s^{-1} at true strain control by means of a MTS extensometer. Reduction of friction between sample and the steel plates was achieved by the application of a thin film PTFE tape between the polymer sample and

the steel plate. Additionally, the contact area between the plate and the tapes was lubricated using a soap-water mixture. As a result, no bulging of the sample was observed during testing. Tensile tests were performed on a Zwick Z010 tensile test machine at constant linear strain rates of 10^{-4} s^{-1} to 10^{-2} s^{-1} . To obtain true stress data, volume invariance was assumed. Creep testing was performed on a long-term dead-weight setup at room temperature. Fatigue experiments were performed on a servo-hydraulic MTS Elastomer Testing System 810. The prescribed stress signal resembles a saw-tooth shape, as depicted in figure 1. Around a mean stress value σ_{mean} , an stress amplitude σ_d was applied with a frequency of 1 Hz. Typically for a set of fatigue experiments, the amplitude stress was taken constant and thus the mean stress was varied.

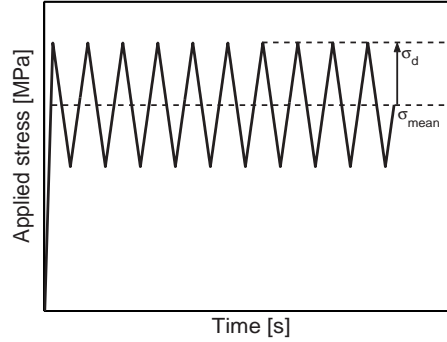


Figure 1: Schematic representation of applied fatigue stress signal

3 NUMERICAL METHODS

3.1 Constitutive modeling

The most important function used in the applied elasto-viscoplastic model is the viscosity function η . In the isothermal case, this function depends on the equivalent shear stress τ_{eq} and the hydrostatic stress p . In this description, the strain softening behavior is governed by parameter D .

$$\eta(\tau_{eq}, D, p) = A_0 \tau_0 \cdot \exp\left(\frac{\mu p}{\tau_0} - D\right) \frac{\tau_{eq}/\tau_0}{\sinh(\tau_{eq}/\tau_0)} \quad (1)$$

where A_0 and τ_0 are parameters from the Eyring-flow relation. The parameter D is increased by aging and decreased by strain softening (evolution of γ_{pl}). These contributions are regarded separately

$$D(t, T, \gamma_{pl}) = D_a(t, T) \cdot g_s(\gamma_{pl}) \quad (2)$$

The softening function g_s is expressed as

$$g_s(\gamma_{pl}) = (1 + (s_0 \cdot \exp(\gamma_{pl}))^{s_1})^{\frac{s_2 - 1}{s_1}} \quad (3)$$

3.2 Incorporation of aging kinetics

Yield stress and softening behavior are strongly related to the thermo-mechanical history as can be seen in figure 2. In this approach, the thermo-mechanical history of the material is captured by the parameter D_a , as already presented in equation 2. The value of this parameter is defined equal to zero in the case of a fully rejuvenated material. Since this parameter is directly related to the yield

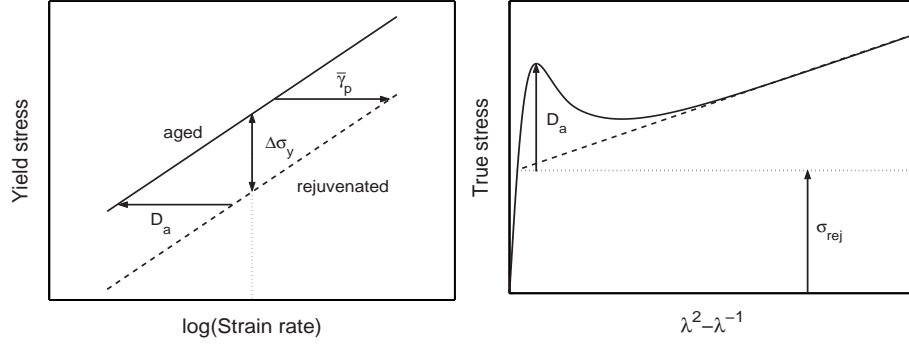


Figure 2: Thermal history captured by a single parameter: D_a

stress, it can simply be determined by a tensile test (Figure 2b). In the case of long-term loading conditions, however, this parameter D_a changes during the experiment due to the so-called progressive aging [7]. To implement this behavior in the numerical model, it is essential to study the aging kinetics as function of stress and temperature. Results will be discussed in chapter 4.

4 RESULTS

4.1 Intrinsic deformation behavior

The modelling parameters were determined from the intrinsic deformation behavior obtained by uni-axial compression testing at true strain rates of 10^{-2} s^{-1} , 10^{-3} s^{-1} and 10^{-4} s^{-1} . Using this procedure, particularly care is taken to accurately capture the materials post-yield behavior. Therefore, a modified Carreau-Yassuda relation [9] is used to phenomenologically describe the softening behavior, as expressed in equation 3. The strain hardening modulus is taken from a study by Tervoort and Govaert [10]. It is emphasized that the parameter set presented in table 1 covers a broad range of molecular weight grades of polycarbonate. In figure 2a, it is shown that the model is able to provide an excellent description of the intrinsic deformation behavior.

POLYCARBONATE		
E	900	[MPa]
ν	0.4	[-]
A_{rej}	$3 \cdot 10^{11}$	[s]
τ_0	0.7	[MPa]
μ	0.08	[-]
D_a	state param.	[-]
s_0	0.965	[-]
s_1	50	[-]
s_2	-5	[-]
G_r	26	[MPa]

Table 1: Material parameters from fitting procedure

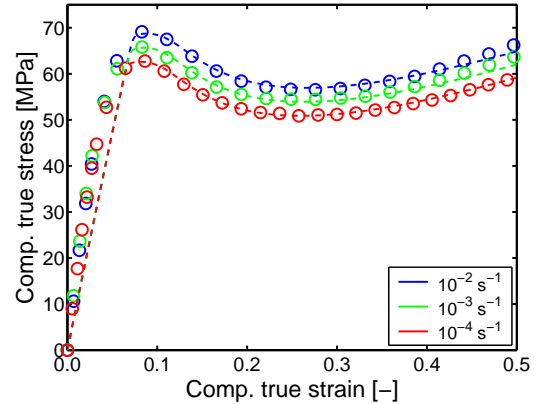


Figure 2a: Verification numerical model on intrinsic deformation behavior of PC

4.2 Aging kinetics

The evolution of D_a is studied by annealing injection molded Lexan 161R samples at elevated temperatures (80-130°C) for a different periods of time. Subsequently, the samples were cooled slowly to room temperature and tested in tensile at 10^{-2} s^{-1} . As shown in figure 2b, the state parameter

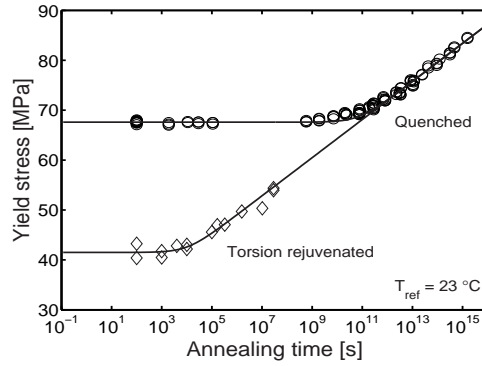


Figure 3: Evolution of yield stress in time for rejuvenated and quenched PC

D_a can be determined from the yield stress. Using an Arrhenius relation, the yield stresses obtained from different temperatures can be shifted to a master curve for specific reference temperature. This resulted in a activation energy of 205 kJ/mole. In addition, the influence of applied stress was studied on injection molded Lexan 161R samples at 80°C. After a specific time of applying a constant load, the sample was unloaded, slowly cooled to room temperature and tensile tested at 10^{-2} s^{-1} to determine its yield stress. This time, a master curve is constructed for a reference load of 0 MPa at 80° using a relation of the Eyring type. The obtained activation volume showed to be $0.77 \text{ m}^3/\text{mole}$. If the obtained master curves are shifted to room temperature, the evolution of the yield stress can be observed over a very wide range of time, see figure 3. From this figure, it can be observed that initially no increase in yield stress occurs. This inactive period is apparently related to the thermal history of the sample. As long as the experimental time is smaller than this initial age $t_{a,i}$, no increase in yield stress will be observed. Only for fully rejuvenated samples, onset of aging is expected to occur immediately. In this approach, the evolution of yield stress σ_y and state parameter D_a , respectively, are described by

$$\sigma_y(t, t_a, T, \sigma) = \sigma_{y,0} + c \cdot \log(t_{eff}(T, \sigma) + t_a) \quad (4)$$

$$D_a(t, t_a, T, \sigma) = c_0 + c_1 \cdot \log(t_{eff}(T, \sigma) + t_a) \quad (5)$$

Moreover, experiments at other grades of PC showed that molecular weight do not affect the aging kinetics. This can be explained from the fact that yield stress is associated to molecular motion and therefore not expected to be affected by molecular weight.

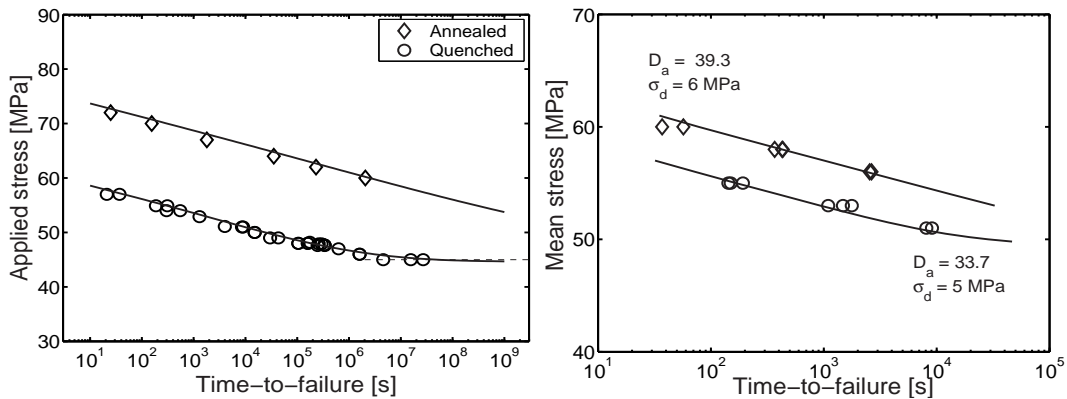


Figure 4: Creep life-time predictions vs. experimental results of quenched and annealed PC (left) Fatigue life-time predictions vs. experimental results for PC (right)

4.3 Application to long-term loading

Validation of the model for long-term loading was initially performed under constant load conditions. Creep experiments were performed on quenched and annealed Lexan 121 samples, see filled circles in figure 4 left). In this figure, the time-to-failure for various stress levels is plotted. Here, time-to-failure is defined as the moment at which macroscopic strain localization (necking) is observed. It is obvious that the annealed samples are able to withstand higher stress levels compared to the quenched samples. To predict the time-of-failure, it is necessary to determine the state parameter D_a to obtain the materials initial age t_a . This is achieved by tensile testing at 10^{-2} s^{-1} . In figure 4 (left), the solid lines are the results of the numerical modelling. For both the quenched and annealed samples, the model is able to predict the time-to-failure quite accurate. Moreover, in the case of the quenched material, the model predicts an endurance limit. A stress level below which no strain localization occurs. Fatigue loading experiments were carried out on PC samples with an amplitude of 5 MPa. In addition, PC samples having a different thermo-mechanical history were subjected to a cyclic loading with an amplitude of 6 MPa. Again, first the state parameter D_a was determined by a simple tensile test to obtain the initial age of the material. The experimental and numerical results are shown in figure 4 (right). These results show to be very promising for the model's abilities to predict time-to-failure, also under cyclic loading conditions.

References

- [1] Haward R. and Thackray G., Proc. Roy. Soc. A, **302**, 453-472 (1968)
- [2] Boyce M.C., Parks D.A., Argon A.S., Mech. Mat., **7**, 15-33 (1988)
- [3] Wu P.D. and van der Giessen E., Mech. Phys. Solids, **41**, 427-456 (1993)
- [4] Buckley C.P. and Jones D.C., Polymer, **36**, 3301-3312 (1995)
- [5] Govaert L.E., Timmermans P.H.M., Brekelmans W.A.M., J. Eng. Mat. Tech., **122**, 177-185 (2000)
- [6] van Melick H.G.H., Govaert L.E., Meijer H.E.H., Polymer, **44**, 3579-3591 (2003)
- [7] Struik L.C.E., *Physical aging in amorphous polymers and other materials*, Elsevier, Amsterdam (1978)
- [8] Klompen E.T.J., Engels T.A.P., Govaert L.E., Meijer H.E.H., submitted to J. Rheol (2004)
- [9] Macosko C.W., *Rheology; Principles, Measurements and Applications.*, VCH Publishers, New York (1994)
- [10] Tervoort T.A. and Govaert L.E., J. Rheol., **44**, 1262-1277 (2000)